Ozone Destruction in Continental Stratus Clouds: An Aircraft Case Study

ZHIEN WANG AND KENNETH SASSEN

Department of Meteorology, University of Utah, Salt Lake City, Utah

(Manuscript received 27 June 1998, in final form 20 July 1999)

ABSTRACT

Apparent depletion of ozone in a cold (~0°C), continental stratus cloud system was observed during in situ data collection on 30 April 1994 at the Department of Energy Clouds and Radiation Test Bed site in northern Oklahoma. Analyses of the aircraft data show a significant negative correlation between ozone concentration and liquid water content (LWC) in this cloud. Although droplets of pure water should not significantly affect ozone concentrations, water clouds can potentially perturb ozone through a number of processes, including radiative effects and aqueous-phase reactions in impure cloud droplets. A simple diagnostic model that takes account of cloud effects on the vertical ozone distribution in the boundary layer was constructed to interpret the field data. The results of multifactor regression analysis indicate that aqueous-phase chemistry contributes predominantly to the negative correlation. A depletion of ozone as a function of LWC of about −6.1 ppbv (g m^{-3})$^{-1}$ was found in this particular stratus. In this case, the average in-cloud reduction of ozone is ~6% for an average LWC of ~0.3 g m^{-3} and ozone mixing ratio of ~31 ppbv outside the cloud layer, which is in reasonable agreement with recent model results.

1. Introduction

There is considerable interest in studying tropospheric ozone (O_3) because of its role as a greenhouse gas and as a key element in tropospheric chemistry. Within the troposphere, ozone is supplied by transport from the stratosphere (Junge 1962; Shapiro 1980; Ancellet et al. 1994), is removed by deposition to the surface (Galbally and Roy 1980; Garland et al. 1980), and is produced and consumed through gas-phase photochemical reactions (Chameides and Walker 1973; Fishman et al. 1979) and heterogeneous chemical reactions (Lelieveld and Crutzen 1990; Jonson and Isaksen 1993; Jacob 1986, 2000), particularly in the planetary boundary layer. These complex chemical and physical processes, which play an important role in the global ozone budget, are incompletely understood. A better understanding of tropospheric ozone requires improved knowledge of the role of the individual chemical and physical processes.

Clouds, where numerous chemical reactions occur, are of great importance to tropospheric chemistry. The uptake of surface-emitted trace gases takes place mostly in clouds, and precipitating clouds return particulate matter and water-soluble gases to the earth's surface. Furthermore, clouds, through scattering, enhance the effect of photochemically active ultraviolet solar radiation. Heterogeneous chemistry involving reactions in aerosols and cloud droplets can affect O_3 concentration in a number of ways, however, including the direct loss of O_3, production and loss of nitrogen oxide radicals [NO_x = nitric oxide (NO) + nitrogen dioxide (NO_2)] and hydrogen oxide radicals [HO_x = hydroxyl (OH) + peroxy radicals], loss of formaldehyde (CH_2O), and the production of halogen radicals (Jacob 2000). Although the role of cloud chemistry in perturbing O_3 concentrations is limited by the small atmospheric volume actually occupied by clouds, the results of model studies nonetheless show that aqueous-phase chemistry can decrease ozone concentrations significantly in the troposphere (Jacob 1986, 2000; Lelieveld and Crutzen 1990, 1991; Liang and Jacob 1997; Matthijsen et al. 1997; Jonson and Isaksen 1993; Walcek et al. 1997). Although the amount of simulated ozone decrease due to heterogeneous cloud chemistry is different in the models used in these various studies, the trend is the same.

Unfortunately, there is a lack of field evidence for the effect of heterogeneous O_3 chemistry in clouds. Direct observation of the perturbation of O_3 from heterogeneous chemistry would require a large effect, and it could be difficult to separate dynamical from chemical effects. On the other hand, Reichardt et al. (1996) and Sassen et al. (1998) have reported pronounced O_3 minima at high altitudes in the presence of cirrus clouds and attributed these minima to heterogeneous chemistry. No evidence for ozone depletion in lower-level clouds has been found previously (Jacob 2000), however. In the current work, evidence for a negative correlation

Corresponding author address: Kenneth Sassen, 135 S 1460 E (819 WBB), University of Utah, Salt Lake City, UT 84112.
E-mail: ksassen@met.utah.edu

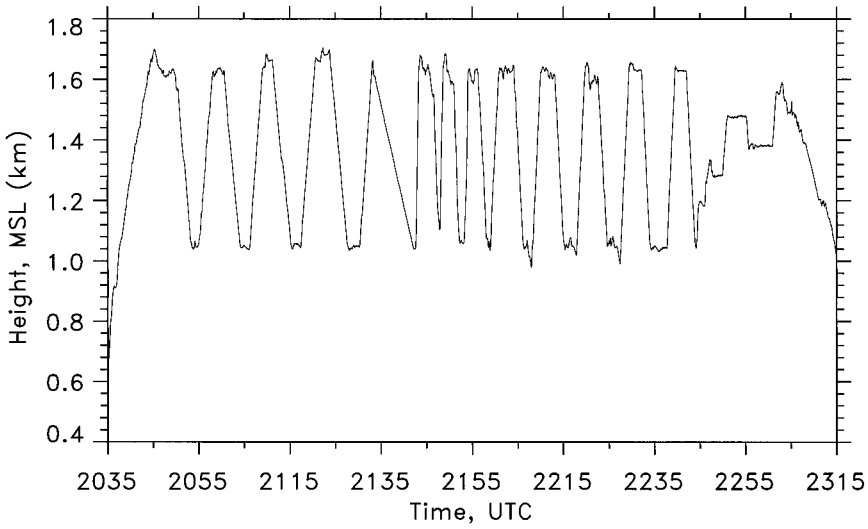

FIG. 1. Time–altitude plot of the University of North Dakota Citation aircraft operations on 30 Apr 1994 in the vicinity of the CART site.

between ozone concentration and liquid water content (LWC) in a continental stratus layer is reported for the first time. Detailed analysis of extensive in situ data will show the magnitude of the effect of heterogeneous chemistry on O_3 concentration.

The organization of the paper is as follows. In section 2, the experiment and aircraft instrumentation are described briefly. In section 3, the theoretical background for this data analysis approach is presented. The effects of cloud-related processes on the ozone distribution are reviewed, and a linear diagnostic model is constructed for the interpretation of the data. The analysis of ozone concentration data collected in situ from a widespread continental stratus cloud system is presented in section 4. The regression method of multifactors is used to analyze the data based on the diagnostic model. The results show strong evidence of ozone depletion due to heterogeneous chemistry in clouds, and the depletion of ozone due to heterogeneous chemistry is calculated. Conclusions are drawn in the final section.

2. Field experiment

This case study is based on aircraft measurements obtained by the University of North Dakota Citation aircraft during the April 1994 Remote Cloud Sensing Intensive Observation Period (RCS IOP) at the Atmospheric Radiation Measurement Program Clouds And Radiation Test Bed (CART) site near Lamont, Oklahoma (Stokes and Schwartz 1994). The goal of the RCS IOP field campaign was to provide closely coordinated air-truth cloud microphysical data for the testing of remote sensing cloud retrieval algorithms under various conditions. As described below, the Citation provided not only state parameters and cloud microphysical data but also ozone concentrations.

The in situ O_3 monitor used on the Citation was a Scintrix chemiluminescent (CL) analyzer. The CL device with eosin is effective for measuring ambient ozone at a high-response frequency (up to 7 Hz) and a detection limit of 0.2 ppb ozone (Ray et al. 1986). Other atmospheric species, including water vapor, produce no interference. Intercomparisons with a UV absorption ozone analyzer showed that rain and high humidity do not change the instrument response (Ray et al. 1986). The CL O_3 analyzer used in this experiment was not calibrated on a daily basis, and so its absolute accuracy is uncertain because of the effects of relatively small drifts between calibrations. Nonetheless, because relative changes in O_3 concentration on any given flight should be reasonably accurate (M. R. Poellot 1998, personal communication), these data appropriately can be used to analyze the effects of clouds on ozone.

The stratus clouds studied on the afternoon of 30 April 1994 were associated with a widespread springtime cold-air outbreak over the central United States. A detailed remote sensing and in situ case study of this cloud has been reported by Sassen et al. (1999). The aircraft measurements consisted of a slow spiral ascent through the stratus cloud deck; a series of ramp climbs and descents; level flight legs near the bottom, middle, and top of the cloud layer; and a final spiral descent over the CART site. The altitude profile of the flight is shown in Fig. 1 and was designed to provide a series of vertical cloud content profiles. The LWC profiles used here were measured by the Forward-Scattering Spectrometer Probe (FSSP) and were in reasonable agreement with those of an independent LWC measurement by a King probe. The vertically integrated liquid water path (LWP) derived from FSSP, however, tends to be ~20% lower than that deduced from a remote sensing algorithm using K_0-band radar and a dual-channel mi-

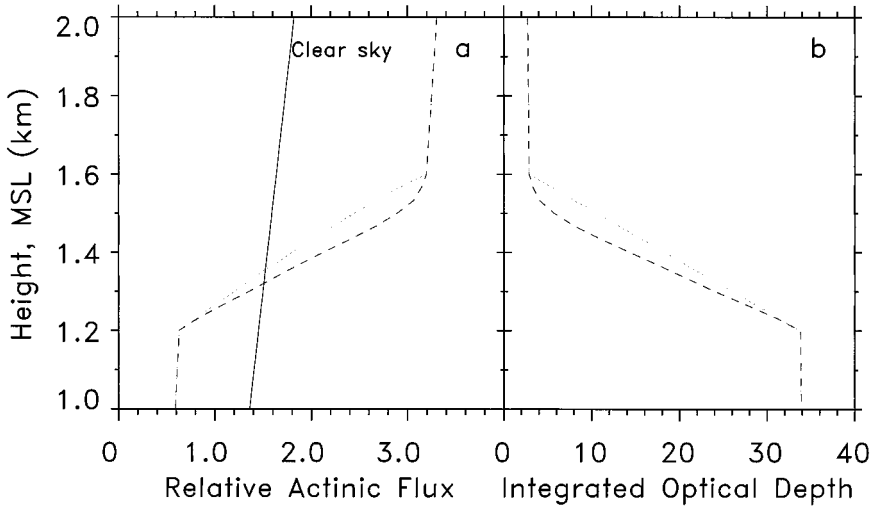

FIG. 2. The effects of cloud on the actinic flux: (a) the relative actinic flux for vertically inhomogeneons (long dashed) and homogeneous (short dashed) clouds, and (b) the corresponding distribution of integrated optical depth.

crowave radiometer (MWR). The possible sources of error in the LWC measurements have been discussed in Sassen et al. (1999) but do not significantly affect our results. Therefore, this field experiment has provided not only an opportunity to understand better the composition and structure of a continental stratus cloud system but also lends itself to understanding the effects of clouds on tropospheric ozone.

3. Effects of clouds on tropospheric ozone: Theory

a. Radiative cloud effects

The chemistry of the atmosphere is driven by solar radiation, which dissociates certain molecules into reactive atoms or free radicals. Models of atmospheric chemistry must include an accurate description of these photodissociation rate coefficients (the J values). For each photoactive molecule having an absorption cross section $\sigma(\lambda)$ and photodissociation quantum yield $\varphi(\lambda)$, the J value is given by integrating the product $\sigma(\lambda)\varphi(\lambda)F(\lambda)$ over the wavelength-range, where $F(\lambda)$ is the actinic flux. In the troposphere, ozone production generally is limited by the availability of NO_x (Chameides et al. 1992), and, in particular, ozone concentration is related closely to the photodissociation rate coefficient of NO_2 (J_{NO_2}) (Weele et al. 1993).

Under cloud-free conditions, solar radiation is affected mainly by gaseous absorption [i.e., O_3 and water (H_2O)], Rayleigh scattering, and aerosol extinction (scattering plus absorption). As compared with cloud-free conditions, clouds significantly disturb the distribution of solar radiation such that clouds affect the actinic flux and, consequently, the ozone distribution.

Theoretical research has addressed the effects of clouds on the photodissociation rate in the troposphere (Madronich 1987; Weele et al. 1993). Weele et al. (1993) studied the effects of clouds on the actinic flux using a multilayer model that calculated the radiation characteristics. The results show that the actinic flux above the clouds is always enhanced relative to the clear-sky values, because the effective albedo of the ground plus cloud is greater than either the ground or cloud albedo alone. The actinic flux below the clouds usually is reduced relative to the clear-sky values. In a homogeneous cloud, the actinic flux changes almost linearly with height in the cloud. Near the cloud top, the flux sometimes is enhanced relative to the actinic flux above the cloud. This enhancement occurs only for high solar elevations when the incoming direct radiation is transmitted more efficiently than is the diffuse radiation. In fact, clouds are inhomogeneous in both the horizontal and vertical directions. The vertical distribution of actinic flux then will be more complex and will depend on the distribution of extinction coefficients within the cloud. Based on the discrete-ordinate radiative transfer (DISORT) code (Stamnes et al. 1988), one can calculate the actinic flux for different situations. Figure 2a shows the relative actinic flux for vertically inhomogeneous (long dashed) and homogeneous (short dashed) clouds, where the solid line is for clear-sky. Figure 2b shows the corresponding distribution of integrated cloud optical depth. A single-scattering albedo of 0.999 and an asymmetry factor of 0.85 were used in these calculations. The vertically inhomogeneous extinction profile is estimated from the stratus-cloud aircraft measurements, and the homogeneous extinction profile is generated with the average extinction coefficient of the inhomogeneous case so that both cases have the same total cloud optical depth. A difference in the vertical actinic flux distributions is obvious for vertically inhomogeneous and homogeneous clouds.

The actinic flux above and below clouds depends pri-

TABLE 1. Important gas-phase and aqueous-phase reactions regulating O_3 concentrations. Here, h is Planck's constant and ν is frequency, denoting a photochemical reaction. The symbol M denotes a species such as oxygen (O_2) that dissipates collision energy.

Gas-phase reactions		Rate constant*
G1	$HO_2 + NO \rightarrow OH + NO_2$	$3.7 \times 10^{-12} \exp(240/T)$
G2	$NO_2 + h\nu \rightarrow NO + O$	5.6×10^{-3}
G3	$O + O_2 + M \rightarrow O_3 + M$	1.5×10^{-15}
G4	$HO_2 + O_3 \rightarrow OH + 2O_2$	$1.1 \times 10^{-14} \exp(-500/T)$
Aqueous-phase reactions		Rate constant (mol^{-1} L s^{-1})
A1	$HO_2 + O_2^- \rightarrow H_2O_2 + O_2 + OH^-$	8.40×10^7
A2	$HO_2 + HO_2 \rightarrow H_2O_2 + O_2$	6.52×10^5
A3	$O_2^- + O_3 + H_2O \rightarrow OH + 2O_2 + OH^-$	1.26×10^9
A4	$HO + HO_2 \rightarrow H_2O + O_2$	5.87×10^9

* Reaction rate constants of first-order reactions: s^{-1}, second-order reactions: molecule^{-1} cm^3 s^{-1}.

marily on cloud optical thickness and solar zenith angle. Solar zenith angle largely controls the shape of the profile with height, and the cloud optical depth mainly affects the magnitudes of the reduction below and the enhancement above the cloud.

Recently, Matthijsen et al. (1997) studied cloud effects on tropospheric ozone on a regional scale with a photochemical dispersion model, LOTOS (Long-Term Ozone Simulation). These model results show that the radiative cloud effect causes a reduction in the O_3 concentration in comparison with clear-sky runs under virtually all circumstances. The radiative cloud effect on O_3 concentration consists of a reduction that depends almost linearly on LWP.

b. Aqueous-phase chemistry

In addition to the direct radiative effect of clouds, a series of aqueous-phase reactions in cloud droplets will disturb the gas-phase reactions and finally affect the distribution of ozone in water clouds (Jacob 1986, 2000; Lelieveld and Crutzen 1990, 1991; Liang and Jacob 1997; Jonson and Isaksen 1993; Walcek et al. 1997). Table 1 only lists several important gas-phase and aqueous-phase reactions, which are the main channels for cloud effects on tropospheric ozone. The rate constants of gas-phase reactions are cited from Leliveld and Crutzen (1991), and aqueous-phase reactions from Walcek et al. (1997). Jacob (1986, 2000), Lelieveld and Crutzen (1990, 1991), Jonson and Isaksen (1993), and Walcek et al. (1997) provide more complete lists and discussions of gas-phase and aqueous-phase reactions related to tropospheric ozone chemistry. From Table 1, it is seen that aqueous-phase reactions are much faster than gas-phase reactions, but the rate of ozone production or removal also depends on the concentration of the reactants. In comparison with gas-phase reactions, aqueous-phase reactions can be regarded as approximately in steady state.

Aqueous-phase chemistry can affect tropospheric ozone in two different ways: a direct loss of ozone in the aqueous phase and an indirect loss of ozone through the effects on gas-phase chemistry. Although ozone has a low solubility in water, which allows for only a small fraction to be absorbed in cloud droplets (Utter et al. 1992), the cloud droplet could provide an important sink for tropospheric ozone through aqueous-phase reaction A3 (Lelieveld and Crutzen 1991). The study of Jonson and Isaksen (1993) has shown that the direct loss of ozone in the aqueous phase accounts for about 50% of the reduction resulting from the inclusion of aqueous-phase chemistry. Cloud droplets scavenge hydroperoxy radical (HO_2), and so on, from the gas phase, so that clouds disturb the gas-phase reactions and reduce the production ratio of ozone mainly through reactions G1–G4 (Table 1) in most situations.

Walcek et al. (1997) performed an in-depth sensitivity study concerning the effect of aqueous-phase chemistry on tropospheric ozone. Their results show that the effect of aqueous chemistry depends on many factors. First, aqueous-phase reactions can decrease or increase the formation rate of ozone in the troposphere, depending on the concentrations of NO_x and nonmethane hydrocarbon. Under relatively clean conditions, that is, when NO_x concentrations are less than a few hundred parts per trillion, aqueous-phase reactions can increase the ozone formation rate slightly, but aqueous-phase reactions clearly reduce the ozone formation rate in polluted conditions. Second, the effect of aqueous-phase reactions changes with the pH value and the concentration of trace metals (copper, iron, and manganese) in cloud droplets. The effect of aqueous-phase reactions also depends on LWC and the size of cloud droplets. The higher the surface area–to-volume ratio is, the more efficient the transfer between the interstitial gas and aqueous phase in the cloud is.

Last, although the ozone formation ratio changes with LWC in a very complicated way (Walcek et al. 1997), one can approximate it with a linear function for low-LWC clouds. Thus it is reasonable approximately to express the effect of aqueous-phase reactions on tropospheric ozone in the cold-stratus case with

$$\Delta O_3 \propto \text{LWC}. \quad (1)$$

c. Diagnostic model

It is obvious that the distribution of tropospheric ozone is governed by a chemical and dynamical process, and thus a very complicated system of equations to describe the ozone distribution is needed (Matthijsen et al. 1997). To investigate the effect of boundary layer clouds on ozone, one can make some simplifications to build a linear model for the analysis of field data. If the effect of clouds on the horizontal and vertical transfer is neglected, the ozone distribution in clouds can be expressed approximately as

$$O_3(x, z, t) = O_{3clear}(x, z, t) + Q_{cloud}(x, z, t)\Delta t, \quad (2)$$

where x is horizontal distance, z is height, t is time, Δt is the time of an air parcel in the cloud, $O_{3clear}(x, z, t)$ is the ozone distribution in a cloudless situation, and $Q_{cloud}(x, z, t)$ is the average net ozone production rate from cloud effects.

The effect of clouds on the O_3 distribution results mainly from the radiative (rad) changes in the actinic flux and the effect of aqueous-phase chemistry (aq), which interact with each other. To build a linear model, a first-order approximation is used to simplify Q_{cloud}:

$$Q_{cloud} = Q_{rad} + Q_{aq}, \quad (3)$$

where Q_{rad} and Q_{aq} represent the average net ozone production rates from the cloud radiative effect and the effect of aqueous-phase chemistry, respectively.

If it is assumed that related pertinent gases (NO_x and HO_x) are distributed uniformly within the boundary layer, the vertical distribution of Q_{rad} will depend principally on the distribution of the actinic flux. Under cloudless conditions, the actinic flux is nearly constant in the boundary layer, so the Q_{rad} profile is nearly constant. However, clouds will redistribute the actinic flux, and, to understand this situation, the Q_{rad} profile can be approximated in the following way:

$$Q_{rad} \propto J_{NO_2} \propto \int_z^{top} \sigma_{cl}\, dz, \quad (4)$$

where ''top'' means the cloud top height, and σ_{cl} is the cloud extinction coefficient.

As discussed in the previous section, the effect of clouds on ozone loss due to aqueous phase chemistry depends almost linearly on LWC according to model studies and theoretical analyses, such that

$$Q_{aq} \propto \text{LWC}. \quad (5)$$

If there are no clouds in the boundary layer, the O_3 concentration can be assumed to be well mixed and can be approximated by

$$O_{3clear}(x, z, t) = \beta_1 + \beta_2 z, \quad (6)$$

where the coefficients β_1 and β_2 for clear air are constant for each profile at a given t and x.

Based on the above analysis, the vertical ozone distribution at a given time and location can be expressed approximately in the following way:

$$O_3(z) = \beta_1 + \beta_2 z + \beta_3 \text{LWC}(z) + \beta_4 \int_z^{top} \sigma_{cl}\, dz, \quad (7)$$

where β_3 and β_4 apply to ozone changes due to aqueous-phase chemistry and radiative effects, respectively, and are constants for a given profile. Here, β_3 and β_4 include a Δt term because it is very difficult to estimate the time of a parcel in the cloud for regression analysis. Because the characteristic time for achieving Henry's equilibrium law between the bulk gas phase and droplet surface is on the order of minutes, we assume a pseudosteady-state of aqueous-phase chemical reactions is achieved here.

In this diagnostic model, the effect of clouds on ozone concentration simply is parameterized as a linear function of LWC and cloud extinction, and any dynamical effects associated with the cloud are neglected. In reality, the effect of clouds on ozone concentration is a nonlinear function of LWC and the abundance of possible species reacting with ozone (Jacob 1986; Walcek et al. 1997). The coefficients β_1, β_2, β_3, and β_4, which are functions of the abundance and distribution of reactive gaseous species and the residence time of air in the cloud, are regarded simply as constants for a given profile. In addition to the radiative effect of clouds, aqueous-phase chemistry in clouds can consume ozone directly and suppress ozone production mechanisms via gas-phase chemistry. Admittedly, to resolve the details of the processes by which clouds can affect ozone concentration, carefully designed field experiments and more complicated diagnostic models are needed. These experiments and models are beyond the focus of this paper. In the following section, the simple model is used to analyze the effects of clouds on the vertical distribution of ozone in the cloud-topped boundary layer.

4. Data analysis

a. Experimental data

Vertical profiles of temperature T, dewpoint temperature T_D, potential temperature, and relative humidity obtained by the Citation during the slow initial spiral ascent over the CART site from 2031 to 2045 UTC on 30 April 1994 are given in Fig. 3. A strong temperature inversion above the stratus (~1.1–1.6 km) was penetrated by the aircraft. The slope of the temperature profile is very close to the dry adiabatic lapse rate below the cloud and is wet adiabatic in the cloud. Potential temperature is nearly constant below the cloud, but a slight increase occurs within the cloud, a sign of stable conditions. Relative humidity increases almost linearly with height below the cloud base, is nearly constant in the cloud layer, and then quickly decreases in the inversion because of cloud-top entrainment effects. These profiles reveal a classic, well-mixed, cloud-topped

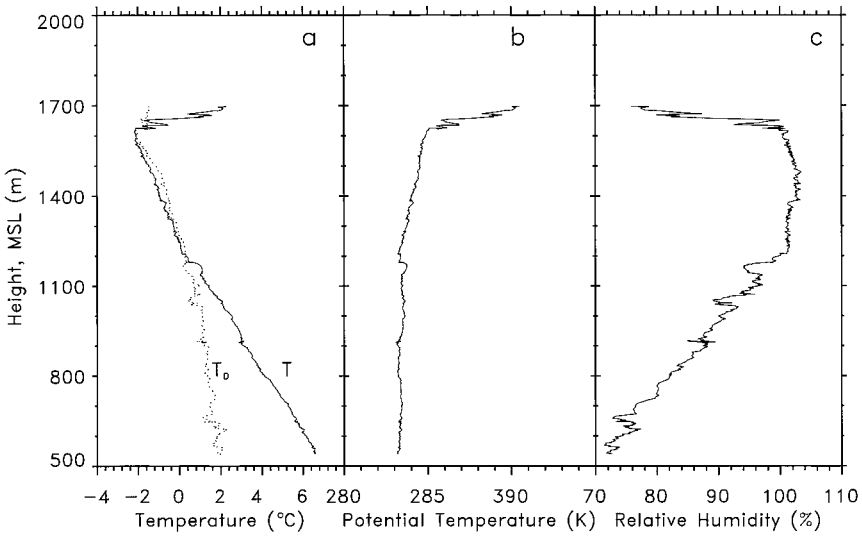

FIG. 3. Profiles of (a) temperature T, dewpoint temperature T_D, (b) potential temperature, and (c) relative humidity obtained by the Citation during the initial spiral ascent (2030–2045 UTC) above the CART site.

boundary layer separated by a strong inversion from the free tropospheric air above.

The examination of the in situ microphysical data begins with Fig. 4, which shows a profile of 30-m-average FSSP mean cloud droplet diameters, also collected during the initial spiral ascent. From Fig. 4 it is seen that the mean droplet diameters remain below ~15 μm, which is very efficient for the mass transfer between the interstitial gas and aqueous phases in the clouds. Also note that the range of vertical velocities measured by the Citation (see Sassen et al. 1999) represents conditions favorable for providing enough time for the interaction of cloud droplet and ozone. These vertical velocities are mostly between ± 25 cm s^{-1}. Although it is difficult to determine how long a particular air parcel would stay in the stratus layer, it is apparent that an air parcel would need at least 1 h to cycle through the ~0.5-km-deep cloud layer, based on the measured magnitudes of the vertical velocities.

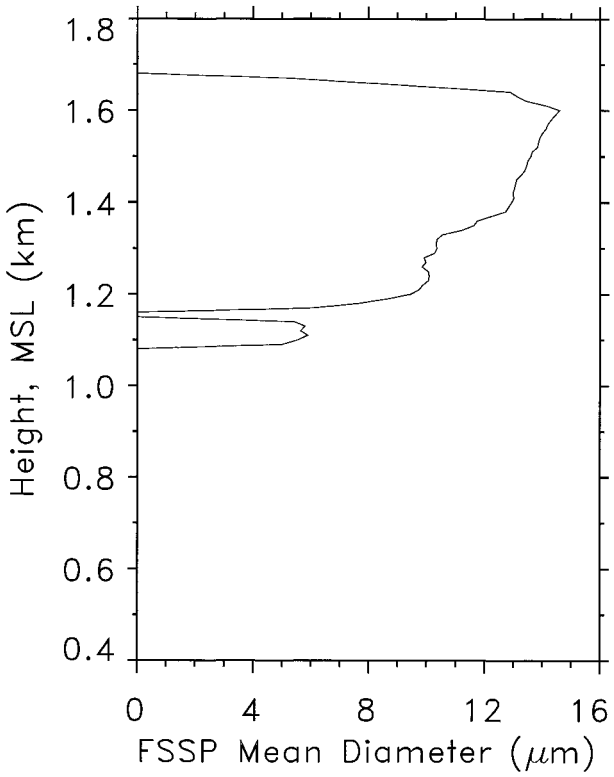

FIG. 4. Vertical profile of the FSSP mean cloud droplet diameter obtained by the Citation during the initial spiral ascent.

As mentioned earlier, the aircraft-supported experiment provided 28 vertical cloud profiles over the 2.5-h Citation mission. In Fig. 5, the profiles of LWC and ozone for each aircraft segment are given. To reduce the impact of LWC variations, these profiles are averaged over 30-m intervals in the vertical direction. From the 27 vertical profiles shown in Fig. 5, it is seen that the stratus layer boundaries range mainly from 1.1 to 1.7 km above mean sea level, LWC extends up to 0.6 g m^{-3}, and the vertical distribution of LWC is somewhat variable with time as the stratus cloud system is evolving. Although the ozone concentration shows a corresponding variability from profile to profile, the relative changes in LWC and O_3 in each profile provide the necessary conditions to examine the effect of water clouds on ozone depletion.

Provided in Fig. 6 is a series of plots of ozone concentration versus LWC derived from each of the vertical profiles. It is obvious that ozone concentration is negatively correlated with LWC for the majority of profiles. Figure 7 shows profiles 2 and 9 in a different manner

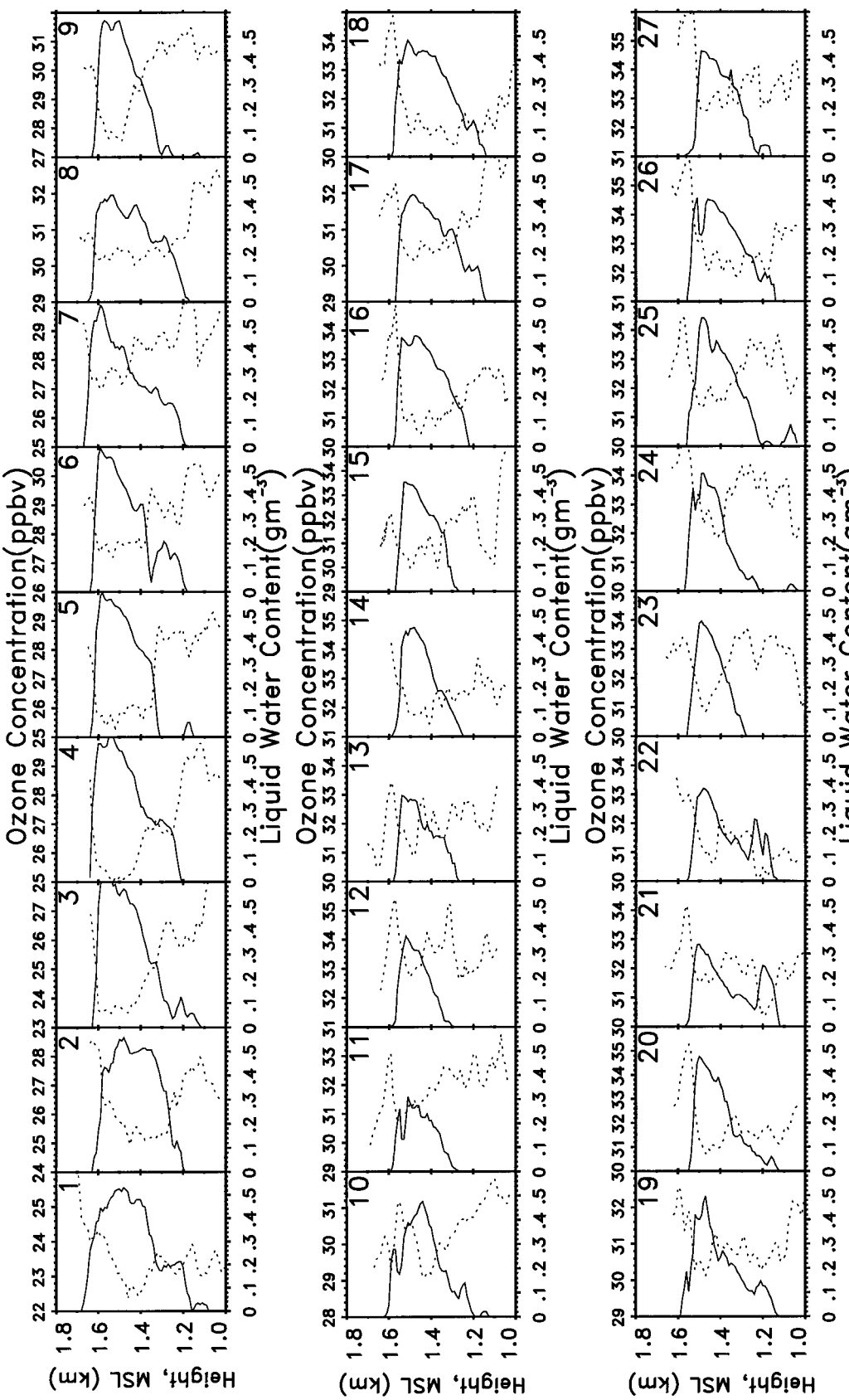

FIG. 5. Vertical profiles of LWC (solid) and O_3 concentration (ppbv) (dashed) corresponding to the first 27 aircraft profiles, using 30-m-averaged height resolution.

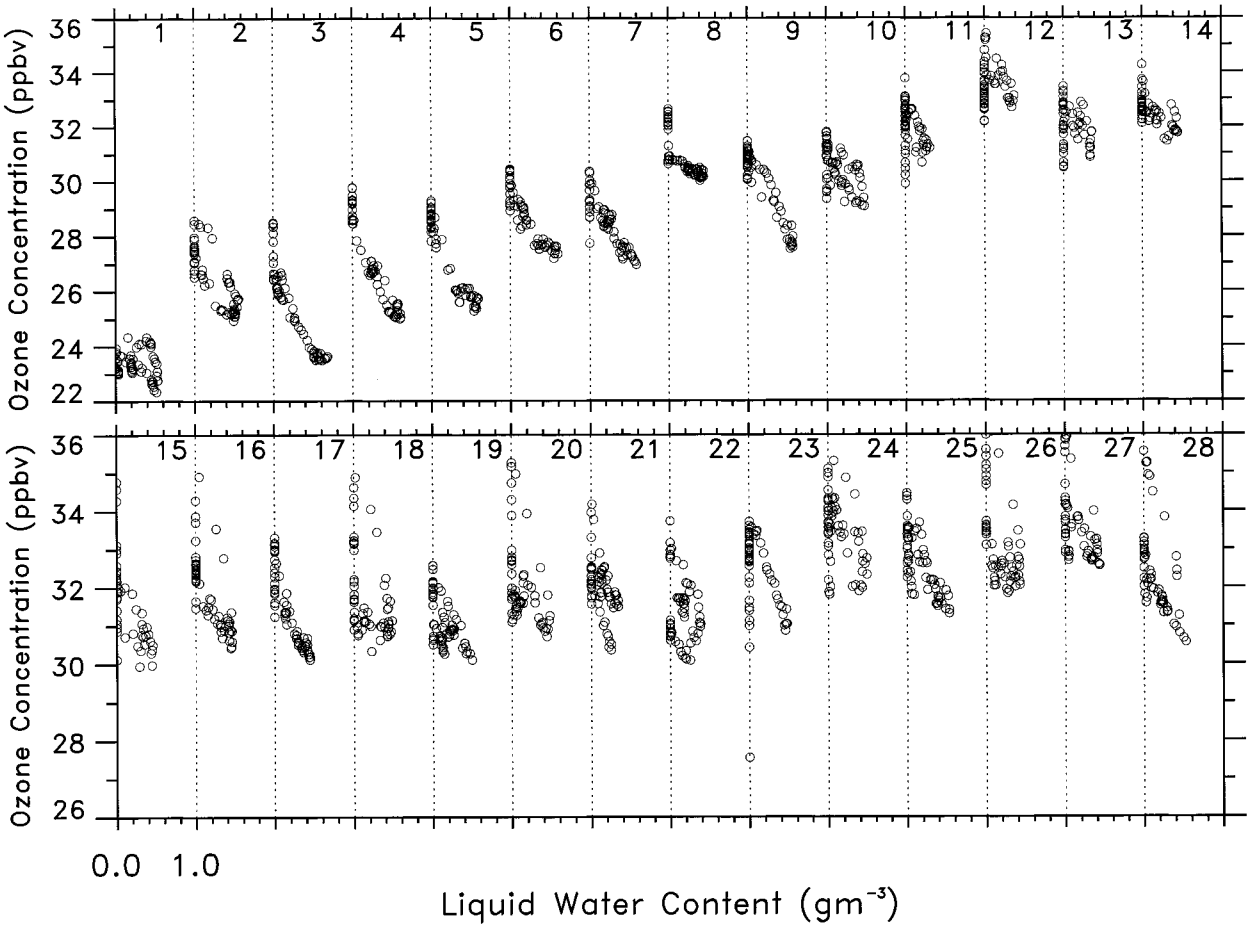

FIG. 6. Plots of O_3 concentration vs LWC for each profile, showing the strong tendency for an O_3 decrease with increasing LWC within the cloud.

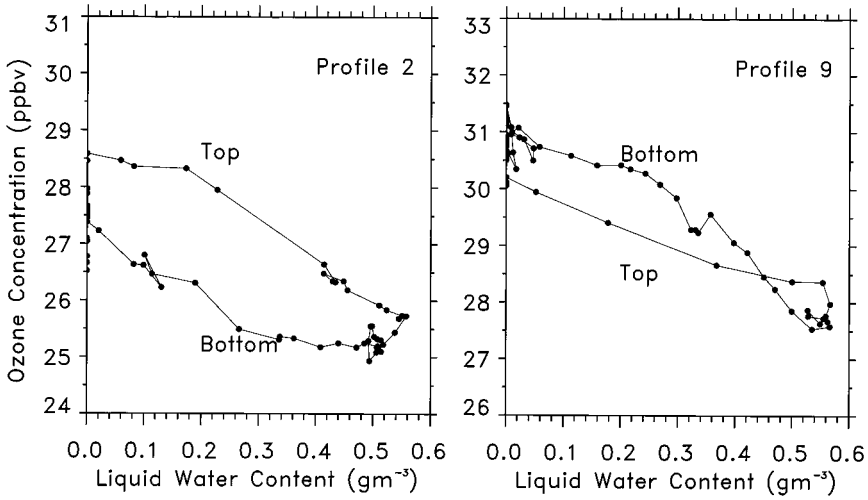

FIG. 7. Expanded views of in situ profiles 2 and 9. Top and bottom refer to the upper and low parts of the cloud, respectively, and each dot symbol is separated by 30-m height intervals.

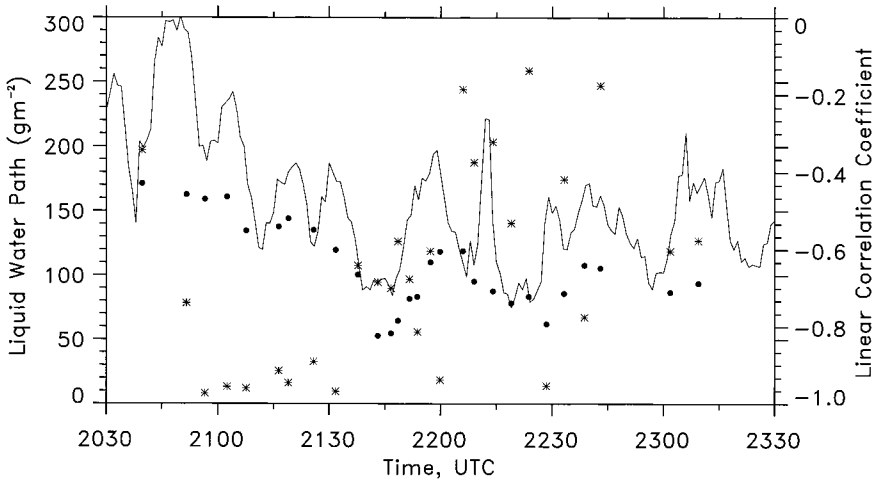

FIG. 8. Changes of LWP (solid line: MWR; dot symbols: aircraft), and the linear correlation coefficients between LWC and O_3 concentration (* symbols) with time over the entire experiment.

(see figure caption); the effects of both the gradual ozone cloud depletion with height and the more-rapid response in the cloud-top entrainment layer are apparent, despite the fact that the surrounding ozone content is somewhat variable. Compared in Fig. 8 are LWP values measured by MWR (solid line) and the vertically integrated aircraft LWC values (dot symbols), along with the linear correlation coefficient between LWC and O_3 concentration (* symbols) for each profile. From these data, it is clear that most correlation coefficients are below -0.5. In the following analysis, we attribute this correlation mostly to the effects of aqueous-phase chemistry. Fig. 9 presents a scatterplot of relative ozone change (with respect to the average ozone concentrations below and above the cloud for each profile) with LWC. The curve fitted to this data (solid line) illustrates that the ozone change is negatively correlated with LWC in the following manner: $\Delta O_3\ (\%) = 0.15 - 14.0(\text{LWC})$.

b. Regression results

Based on the linear diagnostic model described above, the regression method of multifactors can be employed to analyze the effects of clouds on ozone. The ordinary least squares method is applied to determining the coefficients in the diagnostic model [(Eq.) 7], using 30-m-height average ozone and LWC data and a σ_{cl} profile estimated from the LWC profile. Using only data from within the stratus (i.e., LWC > 0) to calculate the model coefficients, values of β and the correlation coefficient R are given in Table 2 for each profile n. The Student's-t statistics for the null hypothesis of $\beta = 0$ are shown in brackets, and ΔZ represents the cloud thickness, from which the number of data points used in each regression analysis can be derived. It can be seen from Table 2 that most of the R values are greater than 80%, indicating that the model can explain most of the ozone changes observed in the stratus layer. For several low-LWP profiles, R is relatively low, suggesting that there may be problems with our assumptions or the in situ data for low LWP.

The clear air coefficients β_1 and β_2 together indicate that the ozone concentration could decrease or increase slightly with height in a well-mixed boundary layer. The small values for β_4 and their unfavorable Student's-t statistics indicate that radiative effects are not a dominant term in Eq. (7). On the other hand, the favorable Student's-t statistics for β_3 suggest that its value is significantly different from zero: all values are negative, thereby supporting the theoretical prediction that liquid water clouds reduce the ozone concentration. In view of the fact that β_3 reflects the importance of aqueous-phase chemistry on the ozone distribution, this fact appears to be the primary reason why the measured ozone concentration is negatively correlated with LWC. The average value of β_3 for R larger than 0.8 is -6.1 ppbv (g m^{-3})$^{-1}$ with a standard error of 2.6. Because this value apparently represents the average O_3 depletion for aqueous-phase chemistry, the magnitude of this effect can be evaluated further.

In the measurements, the average cloud LWC is about 0.3 g m^{-3}, so the average ozone reduction is about 1.8 ppbv, as compared with the average ozone concentration outside the cloud layer of 31 ppbv. Thus, the average reduction in O_3 is about 6%. In comparison with model results, the stratus layer reduced the ozone formation rate by about 1.8 ppbv h^{-1}, assuming Δt is on the order of 1 h and LWC is approximately equal to 0.3 g m^{-3}, which lies within the range of results of Walcek et al. (1997). These experimental results are slightly larger (6% versus 3%–5%) than those of other recent theoretical studies (Liang and Jacob 1997; Matthijsen et al. 1997), but these differences could be attributed to basic differ-

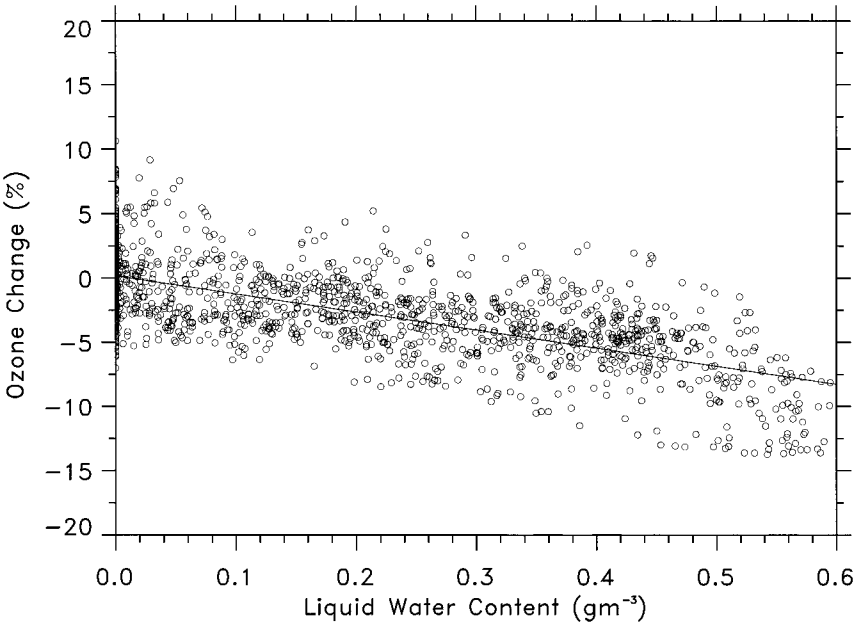

FIG. 9. Scatterplot of O_3 change (relative to the average O_3 concentration above and below the cloud for each profile) with LWC. The solid line provides a fit to the data points (see text).

TABLE 2. Regression results of β values from Eq. (7), and the correlation coefficient R. The Student's-t statistics of β are shown in parentheses.

n	LWP (g m^{-2})	ΔZ (m)	β_1	β_2	β_3	β_4	R
1	171.2	620	24.49 (43.7)	0.52 (0.8)	−2.53 (−8.6)	−0.03 (−2.2)	0.74
2	162.6	420	29.15 (29.6)	−0.30 (−0.3)	−4.98 (−21.5)	−0.06 (−2.3)	0.96
3	159.1	500	26.54 (57.3)	−0.13 (−0.3)	−4.88 (−14.3)	0.00 (−0.1)	0.95
4	160.9	430	30.29 (52.8)	−1.42 (−2.3)	−5.89 (−21.3)	−0.06 (−3.9)	0.96
5	134.4	320	33.51 (15.5)	−5.68 (−2.4)	−3.80 (−5.9)	−0.18 (−2.6)	0.83
6	137.8	450	31.26 (49.4)	−1.57 (−2.4)	−3.85 (−9.4)	−0.05 (−3.0)	0.87
7	144.1	490	31.07 (46.8)	−1.52 (−2.1)	−4.39 (−9.5)	−0.04 (−2.1)	0.90
8	135.1	480	31.79 (70.1)	−0.89 (−1.8)	−1.57 (−9.0)	−0.03 (−1.9)	0.81
9	119.7	360	29.85 (37.3)	0.65 (0.7)	−5.30 (−12.4)	0.05 (1.8)	0.95
10	100.3	480	35.17 (52.2)	−4.82 (−6.5)	−1.05 (−2.4)	−0.17 (−6.4)	0.70
11	52.8	310	30.06 (40.0)	1.39 (1.7)	−2.73 (−4.5)	0.20 (.35)	0.89
12	54.7	310	33.25 (29.1)	2.14 (1.7)	−5.67 (−6.8)	0.06 (0.8)	0.67
13	64.7	310	29.42 (19.1)	3.47 (2.1)	−4.57 (−3.8)	0.20 (2.0)	0.42
14	81.6	330	33.73 (45.3)	−0.38 (−0.5)	−2.68 (−6.8)	−0.06 (−1.6)	0.73
15	83.6	290	33.63 (20.2)	−2.43 (−1.3)	−2.10 (−2.2)	−0.08 (−0.9)	0.73
16	110.1	350	29.50 (25.0)	6.16 (4.7)	−9.41 (−15.9)	0.12 (2.5)	0.92
17	118.5	430	34.45 (56.0)	−2.24 (−3.4)	−4.29 (−15.0)	−0.09 (−3.9)	0.92
18	118.8	440	30.01 (40.5)	5.33 (6.2)	−7.31 (−13.7)	0.05 (1.7)	0.92
19	95.2	510	30.33 (63.6)	1.97 (3.9)	−3.66 (−9.9)	0.02 (0.8)	0.73
20	87.7	420	31.75 (73.1)	3.73 (8.1)	−8.13 (−17.4)	−0.02 (−1.3)	0.90
21	78.3	430	30.15 (48.8)	3.96 (6.7)	−7.35 (−19.8)	0.11 (3.2)	0.94
22	83.3	430	29.32 (32.1)	4.21 (4.6)	−5.61 (−9.6)	0.08 (1.8)	0.82
23	62.1	300	31.26 (122.2)	6.13 (11.5)	−13.36 (−15.2)	0.12 (7.3)	0.99
24	85.9	350	36.13 (49.0)	0.17 (0.2)	−6.48 (−10.5)	−0.11 (−3.2)	0.86
25	107.7	520	30.10 (64.3)	3.52 (7.1)	−4.91 (−11.8)	0.10 (6.3)	0.80
26	105.5	400	33.67 (28.1)	2.58 (2.0)	−7.00 (−8.9)	−0.04 (−0.7)	0.83
27	86.8	390	29.46 (32.3)	6.87 (6.9)	−6.86 (−14.6)	0.19 (4.5)	0.88
28	93.7	540	34.88 (58.9)	1.21 (1.8)	−8.60 (−17.9)	−0.12 (−5.2)	0.91

ences in the cloud microphysical properties measured and modeled, cloud temperature effects, and the assumed concentrations of important gaseous species.

5. Conclusions

Based on in situ data derived from an intensively studied cloud event from the Southern Great Plains CART site, the distribution of ozone in and surrounding an extensive continental stratus cloud layer has been described. A strong negative correlation between ozone concentration and LWC was observed, which appears to depend on both the LWP and the water cloud thickness. The larger the LWP and the thicker the cloud is, the higher the negative correlation is. In contrast, lower LWP values in broken and more transitory clouds are possible reasons that no significant negative correlation has been observed previously in the stratocumulus of the tropical marine boundary layer (Kawa and Pearson 1989), although effects peculiar to continental stratus clouds also may have had an effect. In other words, the effects of cloud lifetime and lateral mixing obviously are important to observing this effect.

In discussing the effects of water clouds on the vertical ozone distribution in the boundary layer, two main processes affecting the ozone distribution have been noted: radiative cloud effects and the effects of aqueous-phase cloud chemistry. For optically homogeneous clouds, the radiative cloud effect changes linearly with cloud depth. The effects of aqueous-phase chemistry, however, depend mainly on the LWC vertical distribution. In the diagnostic model used here to interpret the field data, the effects of clouds have been added to an assumed cloud-free profile. A regression analysis using the multifactor method then was used to calculate the pertinent coefficients in the model. Because all β_3 values are negative with favorable Student's-*t* statistics, the results indicate that aqueous-phase chemistry contributes the most to the negative correlation. The average depletion of ozone in this continental stratus as a function of LWC is estimated to be about -6.1 ppbv (g $m^{-3})^{-1}$, with a standard error of 2.6. It should be noted that this number may be highly variable for different stratus clouds, because the depletion of ozone due to aqueous-phase chemistry in clouds is not only a function of LWC but also of the abundance of a variety of gaseous species that control the ozone production and of the residence time of air in clouds. Although we are uncertain about the relative importance of the direct and indirect ozone depletion processes involving aqueous-phase chemistry, aqueous-phase reactions are considered to be primarily responsible for the measured ozone depletion. In this particular case, the average reduction of ozone measured in situ in the stratus is ~6%, which is in reasonable agreement with recent model results.

Acknowledgments. This research has been supported through the Environmental Sciences Division of the U.S. Department of Energy under Grant DEFG-0394ER61747, as part of the Atmospheric Radiation Measurement Program. The authors thank M. R. Poellot and the anonymous reviewers for their comments.

REFERENCES

Ancellet, G. M., M. Beekmann, and A. Papayannis, 1994: Impact of a cutoff low development on downward transport of ozone in the troposphere. *J. Geophys. Res.,* **99,** 3451–3468.

Chameides, W. L., and J. C. G. Walker, 1973: A photochemical theory of tropospheric ozone. *J. Geophys. Res.,* **78,** 8751–8760.

——, and Coauthors, 1992: Ozone precursor relationships in the ambient atmosphere. *J. Geophys. Res.,* **97,** 6037–6055.

Fishman, J., S. Solomon, and P. J. Crutzen, 1979: Observational and theoretical evidence in support of a significant in-situ photochemical source of tropospheric ozone. *Tellus,* **31,** 432–446.

Galbally, I. E., and C. R. Roy, 1980: Destruction of ozone at the earth's surface. *Quart. J. Roy. Meteor. Soc.,* **106,** 599–620.

Garland, J. A., A. W. Elzerman, and S. A. Penkett, 1980: The mechanism for dry deposition of ozone to seawater surfaces. *J. Geophys. Res.,* **85,** 7488–7492.

Jacob, D., 1986: Chemistry of OH in remote clouds and its role in the production of formic acid and peroxymonosulfate. *J. Geophys. Res.,* **91,** 9807–9826.

——, 2000: Heterogeneous chemistry and tropospheric ozone. *Atmos. Environ.,* **34,** 2131–2159.

Jonson, J. E., and I. S. A. Isaksen, 1993: Tropospheric ozone chemistry: The impact of cloud chemistry. *J. Atmos. Chem.,* **16,** 99–122.

Junge, C. E., 1962: Global ozone budget and exchange between stratosphere and troposphere. *Tellus,* **14,** 363–377.

Kawa, S. R., and R. Pearson Jr., 1989: Ozone budgets from the Dynamics and Chemistry of Marine Stratocumulus experiment. *J. Geophys. Res.,* **94,** 9809–9817.

Lelieveld, J., and P. J. Crutzen, 1990: Influences of cloud photochemical processes on tropospheric ozone. *Nature,* **343,** 227–233.

——, and ——, 1991: The role of clouds in tropospheric photochemistry. *J. Atmos. Chem.,* **12,** 229–267.

Liang, J., and D. J. Jacob, 1997: Effect of aqueous phase cloud chemistry on tropospheric ozone. *J. Geophys. Res.,* **102,** 5993–6001.

Madronich, S., 1987: Photodissociation in the atmosphere, Part 1. Actinic flux and the effects of ground reflections and clouds. *J. Geophys. Res.,* **92,** 9740–9752.

Matthijsen, J., P. Builtjes, E. W. Meijer, and G. Boersen, 1997: Modeling cloud effects on ozone on a regional scale: A case study. *Atmos. Environ.,* **31,** 3227–3238.

Ray, J. D., D. H. Stedman, and G. J. Wendel, 1986: Fast chemiluminescent method for measurement of ambient ozone. *Anal. Chem.,* **58,** 598–600.

Reichardt, J., A. Ansmann, M. Serwazi, C. Weitkamp, and W. Michaelis, 1996: Unexpectedly low ozone concentration in midlatitude tropospheric ice clouds: A case study. *Geophys. Res. Lett.,* **23,** 1929–1932.

Sassen, K., G. G. Mace, J. Hallett, and M. R. Poellot, 1998: Corona-producing ice clouds: A case study of a cold mid-latitude cirrus layer. *Appl. Opt.,* **37,** 1477–1485.

——, ——, Z. Wang, M. R. Poellot, S. M. Sekelsky, and R. E. McIntosh, 1999: Continental stratus clouds: A case study using coordinated remote sensing and aircraft measurements. *J. Atmos. Sci.,* **56,** 2345–2358.

Shapiro, M. A., 1980: Turbulent mixing within tropopause folds as a mechanism for the exchange of chemical constituents between the stratosphere and troposphere. *J. Atmos. Sci.,* **37,** 994–1004.

Stamnes, K., S.-C. Tsay, W. Wiscombe, and K. Jayaweera, 1988: A numerically stable algorithm for discrete-ordinate-method radiative transfer in multiple scattering and emitting layered media. *Appl. Opt.,* **27,** 2502–2509.

Stokes, G. M., and S. E. Schwartz, 1994: The Atmospheric Radiation Measurement (ARM) Program: Programmatic background and design of the Cloud and Radiation Test Bed. *Bull. Amer. Meteor. Soc.,* **75,** 1201–1221.

Utter, R. G., J. B. Burkholder, C. J. Howard, and A. R. Ravishankara, 1992: Measurement of the mass accommodation of ozone on an aqueous surface. *J. Phys. Chem.,* **96,** 4973–4979.

Walcek, C. J., H. Yuan, and W. R. Stockwell, 1997: The influence of aqueous-phase chemical reactions on ozone formation in polluted and nonpolluted clouds. *Atmos. Environ.,* **31,** 1221–1237.

Weele, M. V., and P. G. Duynkerke, 1993: Effect of clouds on the photodissociation of NO_2: Observations and modeling. *J. Atmos. Chem.,* **16,** 231–255.